



**HAL**  
open science

# A Multilevel Schwarz Preconditioner Based on a Hierarchy of Robust Coarse Spaces

Hussam Al Daas, Laura Grigori, Pierre Jolivet, Pierre-Henri Tournier

► **To cite this version:**

Hussam Al Daas, Laura Grigori, Pierre Jolivet, Pierre-Henri Tournier. A Multilevel Schwarz Preconditioner Based on a Hierarchy of Robust Coarse Spaces. *SIAM Journal on Scientific Computing*, 2021, 43 (3), pp.A1907-A1928. 10.1137/19M1266964 . hal-02151184v2

**HAL Id: hal-02151184**

**<https://hal.science/hal-02151184v2>**

Submitted on 7 Dec 2020

**HAL** is a multi-disciplinary open access archive for the deposit and dissemination of scientific research documents, whether they are published or not. The documents may come from teaching and research institutions in France or abroad, or from public or private research centers.

L'archive ouverte pluridisciplinaire **HAL**, est destinée au dépôt et à la diffusion de documents scientifiques de niveau recherche, publiés ou non, émanant des établissements d'enseignement et de recherche français ou étrangers, des laboratoires publics ou privés.

# A MULTILEVEL SCHWARZ PRECONDITIONER BASED ON A HIERARCHY OF ROBUST COARSE SPACES\*

HUSSAM AL DAAS<sup>†</sup>, LAURA GRIGORI<sup>†</sup>, PIERRE JOLIVET<sup>‡</sup>, AND PIERRE-HENRI  
TOURNIER<sup>§</sup>

**Abstract.** In this paper we present a multilevel preconditioner based on overlapping Schwarz methods for symmetric positive definite (SPD) matrices. Robust two-level Schwarz preconditioners exist in the literature to guarantee fast convergence of Krylov methods. As long as the dimension of the coarse space is reasonable, that is, exact solvers can be used efficiently, two-level methods scale well on parallel architectures. However, the factorization of the coarse space matrix may become costly at scale. An alternative is then to use an iterative method on the second level, combined with an algebraic preconditioner, such as a one-level additive Schwarz preconditioner. Nevertheless, the condition number of the resulting preconditioned coarse space matrix may still be large. One of the difficulties of using more advanced methods, like algebraic multigrid or even two-level overlapping Schwarz methods, to solve the coarse problem is that the matrix does not arise from a partial differential equation (PDE) anymore. We introduce in this paper a robust multilevel additive Schwarz preconditioner where at each level the condition number is bounded, ensuring a fast convergence for each nested solver. Furthermore, our construction does not require any additional information than for building a two-level method, and may thus be seen as an algebraic extension.

**Key words.** domain decomposition, multilevel, elliptic problems, subspace correction

**AMS subject classifications.** 65F08, 65F10, 65N55

**1. Introduction.** We consider the solution of a linear system of equations

$$(1.1) \quad Ax = b,$$

where  $A \in \mathbb{R}^{n \times n}$  is a symmetric positive definite (SPD) matrix,  $b \in \mathbb{R}^n$  is the right-hand side, and  $x \in \mathbb{R}^n$  is the vector of unknowns. To enhance convergence, it is common to solve the preconditioned system

$$M^{-1}Ax = M^{-1}b.$$

Standard domain decomposition preconditioners such as block Jacobi, additive Schwarz, and restricted additive Schwarz methods are widely used [32, 9, 8]. In a parallel framework, such preconditioners have the advantage of relatively low communication costs. However, their role in lowering the condition number of the system typically deteriorates when the number of subdomains increases. Multilevel approaches have shown a large impact on enhancing the convergence of Krylov methods [33, 12, 7, 25, 20, 10, 21, 1, 15, 23, 34, 30]. In multigrid and domain decomposition communities, multilevel methods have proven their capacity of scaling up to large numbers of processors and tackling ill-conditioned systems [37, 4, 19]. While some preconditioners are purely algebraic [7, 20, 10, 26, 29, 16, 1], several multilevel methods are based on hierarchical meshing in both multigrid and domain decomposition communities [35, 9, 25, 15, 23]. Mesh coarsening depends on the geometry of the problem. One has to be careful when choosing a hierarchical structure since it can

---

\*Submitted to the editors June 7, 2019.

<sup>†</sup>ALPINES, INRIA, Paris, France (aldaas.hussam@gmail.com, laura.grigori@inria.fr).

<sup>‡</sup>IRIT, CNRS, Toulouse, France (pierre.jolivet@enseeiht.fr).

<sup>§</sup>LJLL, CNRS, Paris, France (tournier@ljl.math.upmc.fr).

40 have a significant impact on the iteration count [23, 25]. In [23], the authors propose  
 41 a multilevel Schwarz domain decomposition solver for the elasticity problem. Based  
 42 on a heuristic approach and following the maximum independent set method [2], they  
 43 coarsen the fine mesh while preserving the boundary in order to obtain a two-level  
 44 method. This strategy is repeated recursively to build several levels. However, they  
 45 do not provide a bound on the condition number of the preconditioned matrix of the  
 46 multilevel method. Multilevel domain decomposition methods are mostly based on  
 47 non-overlapping approaches [35, 9, 25, 23, 37, 4, 30, 34]. Two-level overlapping domain  
 48 decomposition methods are well studied and provide robust convergence estimates  
 49 [33, 12, 5]. However, extending such a construction to more than two levels while  
 50 preserving robustness is not straightforward. In [6], the authors propose an algebraic  
 51 multilevel additive Schwarz method. Their approach is inspired by algebraic multigrid  
 52 strategies. One drawback of it is that it is sensitive to the number of subdomains. In  
 53 [15], the authors suggest applying the two-level Generalized Dryja–Smith–Widlund  
 54 preconditioner recursively to build a multilevel method. In this case, the condition  
 55 number bound of the two-level approach depends on the width of the overlap, the  
 56 diameter of discretization elements, and the diameter of the subdomains. They focus  
 57 on the preconditioner for the three-level case. One drawback of their approach is that  
 58 the three-level preconditioner requires more iterations than the two-level variant. In  
 59 this paper, the only information from the PDE needed for the construction of the  
 60 preconditioner consists of the local Neumann matrices at the fine level. These ma-  
 61 trices correspond to the integration of the bilinear form in the weak formulation of  
 62 the studied PDE on the subdomain-decomposed input mesh. No further information  
 63 is necessary: except on the fine level, our method is algebraic and does not depend  
 64 on any coarsened mesh or auxiliary discretized operator. For problems not arising  
 65 from PDE discretization, one needs to supply the local SPSD matrices on the finest  
 66 level. In [3], a subset of the authors propose a fully algebraic approximation for such  
 67 matrices. However, their approximation strategy is heuristic and may not be effective  
 68 in some cases.

69 Our preconditioner is based on a hierarchy of coarse spaces and is defined as fol-  
 70 lowing. At the first level, the set of unknowns is partitioned into  $N_1$  subdomains and  
 71 each subdomain has an associated matrix  $A_{1,j} = R_{1,j}AR_{1,j}^\top$  obtained by using appro-  
 72 priate restriction and prolongation operators  $R_{1,j}$  and  $R_{1,j}^\top$  respectively, defined in the  
 73 following section. The preconditioner is formed as an additive Schwarz preconditioner  
 74 coupled with an additive coarse space correction, defined as,

$$75 \quad M^{-1} = M_1^{-1} = V_1A_2^{-1}V_1^\top + \sum_{j=1}^{N_1} R_{1,j}^\top A_{1,j}^{-1} R_{1,j},$$

76 where  $V_1$  is a tall-and-skinny matrix spanning a coarse space obtained by solving for  
 77 each subdomain  $j = 1$  to  $N_1$  a generalized eigenvalue problem involving the matrix  
 78  $A_{1,j}$  and the Neumann matrix associated with subdomain  $j$ . The coarse space matrix  
 79 is  $A_2 = V_1^\top AV_1$ . This is equivalent to the GenEO preconditioner, and is described  
 80 in detail in [33] and recalled briefly in section 2. The dimension of the coarse space  
 81 is proportional to the number of subdomains  $N_1$ . When it increases, factorizing  $A_2$   
 82 by using a direct method becomes prohibitive, and hence the application of  $A_2^{-1}$  to a  
 83 vector should also be performed through an iterative method.

84 Our multilevel approach defines a hierarchy of coarse spaces  $V_i$  and coarse space  
 85 matrices  $A_i$  for  $i = 2$  to any depth  $L + 1$ , and defines a preconditioner  $M_i^{-1}$  such that  
 86 the condition number of  $M_i^{-1}A_i$  is bounded. The depth  $L + 1$  is chosen such that the

87 coarse space matrix  $A_{L+1}$  can be factorized efficiently by using a direct method. At  
 88 each level  $i$ , the graph of the coarse space matrix  $A_i$  is partitioned into  $N_i$  subdomains,  
 89 and each subdomain  $j$  is associated with a local matrix  $A_{i,j} = R_{i,j}A_iR_{i,j}^\top$  obtained by  
 90 using appropriate restriction and prolongation operators  $R_{i,j}$  and  $R_{i,j}^\top$ , respectively.  
 91 The preconditioner at level  $i$  is defined as,

$$92 \quad M_i^{-1} = V_i A_{i+1}^{-1} V_i^\top + \sum_{j=1}^{N_i} R_{i,j}^\top A_{i,j}^{-1} R_{i,j},$$

93 where the coarse space matrix is  $A_{i+1} = V_i^\top A_i V_i$ .

94 One of the main contributions of the paper concerns the construction of the  
 95 hierarchy of coarse spaces  $V_i$  for levels  $i$  going from 2 to  $L$ , that are built algebraically  
 96 from the coarse space of the previous level  $V_{i-1}$ . This construction is based on the  
 97 definition of local symmetric positive semi-definite (SPSD) matrices associated with  
 98 each subdomain  $j$  at each level  $i$  that we introduce in this paper. These matrices are  
 99 obtained by using the local SPSPD matrices of the previous level  $i-1$  and the previous  
 100 coarse space  $V_{i-1}$ . They are then involved, with the local matrices  $A_{i,j}$ , in concurrent  
 101 generalized eigenvalue problems solved for each subdomain  $j$  that allows to compute  
 102 the local eigenvectors contributing to the coarse space  $V_i$ .

103 We show in [Theorem 5.3, section 5](#), that the condition number of  $M_i^{-1}A_i$  is  
 104 bounded and depends on the maximum number of subdomains at the first level that  
 105 share an unknown, the number of distinct colors required to color the graph of  $A_i$  so  
 106 that  $\{span\{R_{i,j}^\top\}\}_{1 \leq j \leq N_i}$  of the same color are mutually  $A_i$ -orthogonal, and a user  
 107 defined tolerance  $\tau$ . It is thus independent of the number of subdomains  $N_i$ .

108 The main contribution of this paper is based on the combination of two previous  
 109 works on two-level additive Schwarz methods [\[3, 33\]](#). The coarse space proposed in  
 110 [\[33\]](#) guarantees an upper bound on the condition number that can be prescribed by  
 111 the user. The SPSPD splitting in the context of domain decomposition presented in  
 112 [\[3\]](#) provides an algebraic view for the construction of coarse spaces. The combination  
 113 of these two works leads to a robust multilevel additive Schwarz method. Here,  
 114 robustness refers to the fact that at each level, an upper bound on the condition  
 115 number of the associated matrix can be prescribed by the user a priori. The rest  
 116 of the paper is organized as follows. In the next section, we present the notations  
 117 used throughout the paper. In [section 2](#), we present a brief review of the theory of  
 118 one- and two-level additive Schwarz methods. We extend in [section 3](#) the class of  
 119 SPSPD splitting matrices presented in [\[3\]](#) in order to make it suitable for multilevel  
 120 methods. Afterwards, we define the coarse space at level  $i$  based on the extended  
 121 class of local SPSPD splitting matrices associated with this level. [Section 4](#) describes  
 122 the partitioning of the domain at level  $i+1$  from the partitioning at level  $i$ . In  
 123 [Section 5](#), we explain the computation of the local SPSPD matrices associated with each  
 124 subdomain at level  $i+1$ . We compute them using those associated with subdomains  
 125 at level  $i$ . [Section 6](#) presents numerical experiments on highly challenging diffusion  
 126 and linear elasticity problems in two- and three-dimensional problems. We illustrate  
 127 the theoretical robustness and practical usage of our proposed method by performing  
 128 strong scalability tests up to 8,192 processes.

129 **Context and notation.** By convention, the finest level, on which [\(1.1\)](#) is  
 130 defined, is the first level. A subscript index is used in order to specify which level  
 131 an entity is defined on. In the case where additional subscripts are used, the first  
 132 subscript always denotes the level. For the sake of clarity, we omit the subscript cor-

133 responding to level 1 when it is clear from context, e.g., matrix  $A$ . Furthermore, the  
 134 subscripts  $i$  and  $j$  always refer to a specific level  $i$  and its subdomain  $j$ , respectively.  
 135 The number of levels is  $L + 1$ . Let  $A_i \in \mathbb{R}^{n_i \times n_i}$  denote symmetric positive definite  
 136 matrices, each corresponding to level  $i = 1, \dots, L + 1$ . We suppose that a direct solver  
 137 can be used at level  $L + 1$  to compute an exact factorization of  $A_{L+1}$ .

138 Let  $B \in \mathbb{R}^{p \times q}$  be a matrix. Let  $P \subset \llbracket 1; p \rrbracket$  and  $Q \subset \llbracket 1; q \rrbracket$  be two sets of  
 139 indices. The concatenation of  $P$  and  $Q$  is represented by  $[P, Q]$ . We note that the  
 140 order of the concatenation is important.  $B(P, :)$  is the submatrix of  $B$  formed by  
 141 the rows whose indices belong to  $P$ .  $B(:, Q)$  is the submatrix of  $B$  formed by the  
 142 columns whose indices belong to  $Q$ .  $B(P, Q) = (B(P, :))(:, Q)$ . The identity matrix  
 143 of size  $p$  is denoted  $I_p$ . We suppose that the graph of  $A_i$  is partitioned into  $N_i$  non-  
 144 overlapping subdomains, where  $N_i \ll n_i$  and  $N_{i+1} \leq N_i$  for  $i = 1, \dots, L$ . We note that  
 145 partitioning at level 1 can be performed by using a graph partitioning library such as  
 146 ParMETIS [22] or PT-SCOTCH [11]. Partitioning at greater levels will be described  
 147 later in section 4. In the following, we define for each level  $i = 1, \dots, L$  notations  
 148 for subsets and restriction operators that are associated with the partitioning. Let  
 149  $\Omega_i = \llbracket 1; n_i \rrbracket$  be the set of unknowns at level  $i$  and let  $\Omega_{i,j,I}$  for  $j = 1, \dots, N_i$  be the  
 150 subset of  $\Omega_i$  that represents the unknowns in subdomain  $j$ . We refer to  $\Omega_{i,j,I}$  as the  
 151 *interior unknowns* of subdomain  $j$ . Let  $\Gamma_{i,j}$  for  $j = 1, \dots, N_i$  be the subset of  $\Omega_i$  that  
 152 represents the neighbor unknowns of subdomain  $j$ , i.e., the unknowns at distance 1  
 153 from subdomain  $j$  through the graph of  $A_i$ . We refer to  $\Gamma_{i,j}$  as the *overlapping*  
 154 *unknowns* of subdomain  $j$ . We denote  $\Omega_{i,j} = [\Omega_{i,j,I}, \Gamma_{i,j}]$ , for  $j = 1, \dots, N_i$ , the  
 155 concatenation of interior and overlapping unknowns of subdomain  $j$ . We denote  
 156  $\Delta_{i,j}$ , for  $j = 1, \dots, N_i$ , the complementary of  $\Omega_{i,j}$  in  $\Omega_i$ , i.e.,  $\Delta_{i,j} = \Omega_i \setminus \Omega_{i,j}$ . In  
 157 Figure 1.1, a triangular mesh is used to discretize a square domain. The set of  
 158 nodes of the mesh is partitioned into 16 disjoint subsets  $\Omega_{1,j,I}$ , which represent a  
 159 non-overlapping decomposition, for  $j = 1, \dots, 16$  (left). On the left, a matrix  $A_1$   
 160 whose connectivity graph corresponds to the mesh is illustrated. The submatrix  
 161  $A_1(\Omega_{1,j,I}, \Omega_{1,j,I})$  is associated with the non-overlapping subdomain  $j$ . Each submatrix  
 162  $A_1(\Omega_{1,j,I}, \Omega_{1,j,I})$  is colored with a distinct color. The same color is used to color the  
 163 region that contains the nodes in the non-overlapping subdomain  $\Omega_{1,j,I}$ . Note that  
 164 if two subdomains  $j_1, j_2$  are neighbors, the submatrix  $A_1(\Omega_{1,j_1,I}, \Omega_{1,j_2,I})$  has nonzero  
 165 elements. For  $j = 1, \dots, N_i$ , we denote by  $n_{i,j,I}$ ,  $\gamma_{i,j}$  and  $n_{i,j}$  the cardinality of  $\Omega_{i,j,I}$ ,  
 166  $\Gamma_{i,j}$  and  $\Omega_{i,j}$  respectively.

167 Let  $R_{i,j,I} \in \mathbb{R}^{n_{i,j,I} \times n_i}$  be defined as  $R_{i,j,I} = I_{n_i}(\Omega_{i,j,I}, :)$ .

168 Let  $R_{i,j,\Gamma} \in \mathbb{R}^{\gamma_{i,j} \times n_i}$  be defined as  $R_{i,j,\Gamma} = I_{n_i}(\Gamma_{i,j}, :)$ .

169 Let  $R_{i,j} \in \mathbb{R}^{n_{i,j} \times n_i}$  be defined as  $R_{i,j} = I_{n_i}(\Omega_{i,j}, :)$ .

170 Let  $R_{i,j,\Delta} \in \mathbb{R}^{(n_i - n_{i,j}) \times n_i}$  be defined as  $R_{i,j,\Delta} = I_{n_i}(\Delta_{i,j}, :)$ .

171 Let  $\mathcal{P}_{i,j} = I_{n_i}([\Omega_{i,j,I}, \Gamma_{i,j}, \Delta_{i,j}], :) \in \mathbb{R}^{n_i \times n_i}$ , be a permutation matrix associated  
 172 with the subdomain  $j$ , for  $j = 1, \dots, N_i$ . The matrix of the overlapping subdomain  $j$ ,  
 173  $R_{i,j} A_i R_{i,j}^\top$ , is denoted  $A_{i,j}$ . We denote  $D_{i,j} \in \mathbb{R}^{n_{i,j} \times n_{i,j}}$ ,  $j = 1, \dots, N_i$ , any set of  
 174 non-negative diagonal matrices such that

$$175 \quad I_{n_i} = \sum_{j=1}^{N_i} R_{i,j}^\top D_{i,j} R_{i,j}.$$

176 We refer to  $\{D_{i,j}\}_{1 \leq j \leq N_i}$  as the algebraic partition of unity. Let  $V_i \in \mathbb{R}^{n_i \times n_{i+1}}$  be  
 177 a tall-and-skinny matrix of full rank. We denote  $\mathcal{S}_i$  the subspace spanned by the  
 178 columns of  $V_i$ . This subspace will stand for the coarse space associated with level  $i$ .  
 179 By convention, we refer to  $\mathcal{S}_i$  as subdomain 0 at level  $i$ . Thus, we have  $n_{i,0} = n_{i+1}$ .

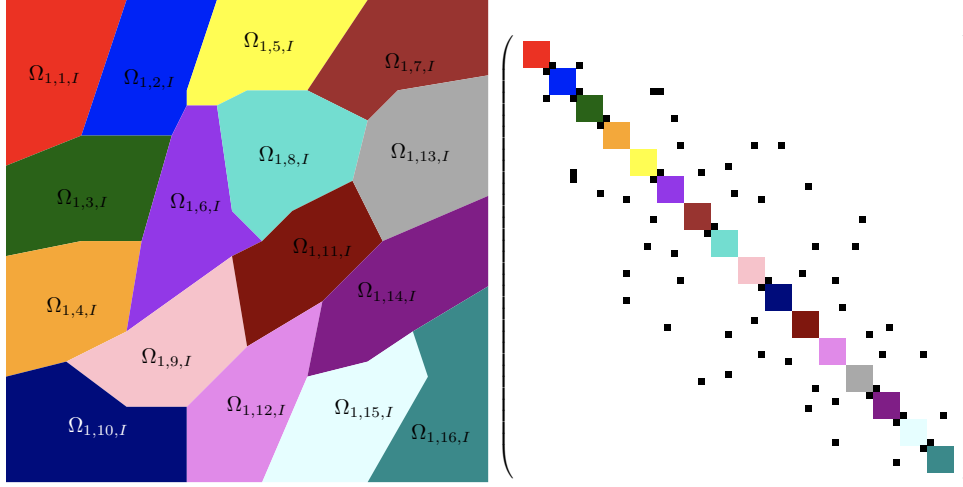


FIG. 1.1. *Left: a triangular mesh is used to discretize the unit square. The set of nodes of the mesh is partitioned into 16 disjoint subsets, non-overlapping subdomains,  $\Omega_{1,j,I}$  for  $j = 1, \dots, 16$ . Right: Illustration of the matrix  $A_1$  whose connectivity graph corresponds to the mesh on the left. The diagonal block  $j$  of  $A_1$  corresponds to the non-overlapping subdomain  $\Omega_{1,j,I}$ . Each submatrix  $A_1(\Omega_{1,j,I}, \Omega_{1,j,I})$  is colored with a distinct color. The same color is used to color the region of the square that contains nodes in  $\Omega_{1,j,I}$ .*

180 The interpolation operator at level  $i$  is defined as:

$$\begin{aligned}
 & \mathcal{R}_{i,2}: \prod_{j=0}^{N_i} \mathbb{R}^{n_{i,j}} \rightarrow \mathbb{R}^{n_i} \\
 & (u_j)_{0 \leq j \leq N_i} \mapsto \sum_{j=0}^{N_i} R_{i,j}^\top u_j.
 \end{aligned}
 \tag{1.2}$$

183 Finally, we denote  $\mathcal{V}_{i,j}$  the set of neighboring subdomains of each subdomain  $j$  at  
 184 level  $i$  for  $(i, j) \in \llbracket 1; L \rrbracket \times \llbracket 1; N_i \rrbracket$ .

$$\mathcal{V}_{i,j} = \{k \in \llbracket 1; N_i \rrbracket : \Omega_{i,j} \cap \Omega_{i,k} \neq \emptyset\}.$$

186 As previously mentioned, partitioning at level 1 can be performed by graph parti-  
 187 tioning libraries such as ParMETIS [22] or PT-SCOTCH [11]. Partitioning at further  
 188 levels will be defined later: the sets  $\Omega_{i,j,I}$ ,  $\Omega_{i,j,\Gamma}$ ,  $\Omega_{i,j}$ , and  $\Delta_{i,j}$  for  $i > 1$  are defined  
 189 in subsection 4.2. The coarse spaces  $\mathcal{S}_i$  as well as the projection and prolongation  
 190 operators  $V_i^\top$  and  $V_i$  are defined in subsection 3.2. We suppose that the connectivity  
 191 graph between the subdomains on each level is sparse. This assumption is not true in  
 192 general, however, it is valid in structures based on locally constructed coarse spaces  
 193 in domain decomposition as we show in this paper, see [18, Section 4.1 p.81] for the  
 194 case of two levels.

195 **2. Background.** In this section, we review briefly several theoretical results  
 196 related to additive Schwarz preconditioners. We introduce them for the sake of com-  
 197 pleteness.

198 LEMMA 2.1 (fictitious subspace lemma). *Let  $A \in \mathbb{R}^{n_A \times n_A}$ ,  $B \in \mathbb{R}^{n_B \times n_B}$  be two*

199 symmetric positive definite matrices. Let  $\mathcal{R}$  be an operator defined as

$$\begin{aligned} 200 \quad & \mathcal{R}: \mathbb{R}^{n_B} \rightarrow \mathbb{R}^{n_A} \\ 201 \quad & v \mapsto \mathcal{R}v, \end{aligned}$$

202 and let  $\mathcal{R}^\top$  be its transpose. Suppose that the following conditions hold:

- 203 1. The operator  $\mathcal{R}$  is surjective.
- 204 2. There exists  $c_u > 0$  such that

$$205 \quad (\mathcal{R}v)^\top A (\mathcal{R}v) \leq c_u v^\top B v, \quad \forall v \in \mathbb{R}^{n_B}.$$

- 206 3. There exists  $c_l > 0$  such that for all  $v_{n_A} \in \mathbb{R}^{n_A}, \exists v_{n_B} \in \mathbb{R}^{n_B} | v_{n_A} = \mathcal{R}v_{n_B}$
- 207 and

$$208 \quad c_l v_{n_B}^\top B v_{n_B} \leq (\mathcal{R}v_{n_B})^\top A (\mathcal{R}v_{n_B}) = v_{n_A}^\top A v_{n_A}.$$

209 Then, the spectrum of the operator  $\mathcal{R}B^{-1}\mathcal{R}^\top A$  is contained in the segment  $[c_l, c_u]$ .

210 *Proof.* We refer the reader to [12, Lemma 7.4 p.164] or [28, 27, 13] for a detailed  
211 proof.  $\square$

212 LEMMA 2.2. The operator  $\mathcal{R}_{i,2}$  as defined in (1.2) is surjective.

213 *Proof.* The proof follows from the definition of  $\mathcal{R}_{i,2}$  (1.2).  $\square$

214 LEMMA 2.3. Let  $k_{i,c}$  for  $i = 1, \dots, L$  be the minimum number of distinct colors  
215 so that  $\{\text{span}\{R_{i,j}^\top\}\}_{1 \leq j \leq N_i}$  of the same color are mutually  $A_i$ -orthogonal. Then, we  
216 have

$$\begin{aligned} 218 \quad & (\mathcal{R}_{i,2}u_{\mathcal{B}_i})^\top A_i (\mathcal{R}_{i,2}u_{\mathcal{B}_i}) \\ 219 \quad & \leq (k_{i,c} + 1) \sum_{j=0}^{N_i} u_j^\top (R_{i,j} A_i R_{i,j}^\top) u_j, \quad \forall u_{\mathcal{B}_i} = (u_j)_{0 \leq j \leq N_i} \in \prod_{j=0}^{N_i} \mathbb{R}^{n_{i,j}}. \end{aligned}$$

221 *Proof.* We refer the reader to [9, Theorem 12 p.93] for a detailed proof.  $\square$

222 We note that at level  $i$ , the number  $k_{i,c}$  is smaller than the maximum number of  
223 neighbors over the set of subdomains  $\llbracket 1; N_i \rrbracket$

$$224 \quad k_{i,c} \leq \max_{1 \leq j \leq N_i} \#\mathcal{V}_{i,j}.$$

225 Due to the sparse structure of the connectivity graph between the subdomains at  
226 level  $i$ , the maximum number of neighbors over the set of subdomains  $\llbracket 1; N_i \rrbracket$  is  
227 independent of the number of subdomains  $N_i$ . Then, so is  $k_{i,c}$ .

228 LEMMA 2.4. Let  $u_{A_i} \in \mathbb{R}^{n_{A_i}}$  and  $u_{\mathcal{B}_i} = \{u_j\}_{0 \leq j \leq N_i} \in \prod_{j=0}^{N_i} \mathbb{R}^{n_{i,j}}$  such that  $u_{A_i} =$   
229  $\mathcal{R}_{i,2}u_{\mathcal{B}_i}$ . The additive Schwarz operator without any other restriction on the coarse  
230 space  $\mathcal{S}_i$  verifies the following inequality

$$231 \quad \sum_{j=0}^{N_i} u_j^\top (R_{i,j} A_i R_{i,j}^\top) u_j \leq 2u_{A_i}^\top A_i u_{A_i} + (2k_{i,c} + 1) \sum_{j=1}^{N_i} u_j^\top R_{i,j} A_i R_{i,j}^\top u_j,$$

232 where  $k_{i,c}$  is defined in Lemma 2.3.

233 *Proof.* We refer the reader to [12, Lemma 7.12, p. 175] to view the proof in  
 234 detail.  $\square$

235 **LEMMA 2.5.** *Let  $A, B \in \mathbb{R}^{m \times m}$  be two symmetric positive semi-definite matrices.*  
 236 *Let  $\ker(A)$ ,  $\text{range}(A)$  denote the null space and the range of  $A$  respectively. Let  $P_0$*   
 237 *be an orthogonal projection on  $\text{range}(A)$ . Let  $\tau$  be a positive real number. Consider*  
 238 *the generalized eigenvalue problem,*

$$239 \quad P_0 B P_0 u_k = \lambda_k A u_k,$$

$$240 \quad (u_k, \lambda_k) \in \text{range}(A) \times \mathbb{R}.$$

241 *Let  $P_\tau$  be an orthogonal projection on the subspace*

$$242 \quad Z = \ker(A) \oplus \text{span}\{u_k \mid \lambda_k > \tau\},$$

243 *then, the following inequality holds:*

$$244 \quad (2.1) \quad (u - P_\tau u)^\top B (u - P_\tau u) \leq \tau u^\top A u, \quad \forall u \in \mathbb{R}^m.$$

245 *Proof.* We refer the reader to [3, Lemma 2.4] and [12, Lemma 7.7] for a detailed  
 246 proof.  $\square$

247 **2.1. GenEO coarse space.** In [33, 12] the authors present the GenEO coarse  
 248 space which relies on defining appropriate symmetric positive semi-definite (SPSD)  
 249 matrices  $\tilde{A}_j \in \mathbb{R}^{n \times n}$  for  $j = 1, \dots, N$ . These are the unassembled Neumann matrices,  
 250 corresponding to the integration on each subdomain of the operator defined in the  
 251 variational form of the PDE. These matrices are local, i.e.,  $R_{j,\Delta} \tilde{A}_j = 0$ . Furthermore,  
 252 they verify the relations

$$u^\top \tilde{A}_j u \leq u^\top A u, \quad \forall u \in \mathbb{R}^n,$$

$$253 \quad u^\top \sum_{j=1}^N \tilde{A}_j u \leq k_{\text{GenEO}} u^\top A u, \quad \forall u \in \mathbb{R}^n,$$

254 where  $k_{\text{GenEO}} \leq N$  is the maximum number of subdomains that share an unknown.

255 **2.2. Local SPSP splitting of an SPD matrix.** In [3], the authors present  
 256 the local SPSP splitting of an SPD matrix. Given the permutation matrix  $\mathcal{P}_j$ , a local  
 257 SPSP splitting matrix  $\tilde{A}_j$  of  $A$  associated with subdomain  $j$  is defined as

$$259 \quad (2.2) \quad \mathcal{P}_j \tilde{A}_j \mathcal{P}_j^\top = \begin{pmatrix} R_{j,I} A R_{j,I}^\top & R_{j,I} A R_{j,\Gamma}^\top \\ R_{j,\Gamma} A R_{j,I}^\top & \tilde{A}_\Gamma^j \\ & & 0 \end{pmatrix},$$

260 where  $\tilde{A}_\Gamma^j \in \mathbb{R}^{\gamma_j \times \gamma_j}$  satisfies the two following conditions: For all  $u \in \mathbb{R}^{\gamma_j}$ ,

- 261  $\bullet u^\top (R_{j,\Gamma} A R_{j,I}^\top) (R_{j,I} A R_{j,I}^\top)^{-1} (R_{j,I} A R_{j,\Gamma}^\top) u \leq u^\top \tilde{A}_\Gamma^j u$
- 262  $\bullet u^\top \tilde{A}_\Gamma^j u \leq u^\top \left( (R_{j,\Gamma} A R_{j,\Gamma}^\top) - (R_{j,\Gamma} A R_{j,\Delta}^\top) (R_{j,\Delta} A R_{j,\Delta}^\top)^{-1} (R_{j,\Delta} A R_{j,\Gamma}^\top) \right) u.$

263 The authors prove that the matrices  $\tilde{A}_j$  defined in such a way verify the following  
 264 relations:

$$265 \quad (2.3) \quad R_{j,\Delta} \tilde{A}_j = 0,$$

$$266 \quad (2.4) \quad u^\top \tilde{A}_j u \leq u^\top A u, \quad \forall u \in \mathbb{R}^n,$$

$$267 \quad (2.5) \quad u^\top \sum_{j=1}^N \tilde{A}_j u \leq k u^\top A u, \quad \forall u \in \mathbb{R}^n,$$

268



269 where  $k$  is a number that depends on the local SPSD splitting matrices and can be  
 270 at most equal to the number of subdomains  $k \leq N$ . The authors also show that the  
 271 local matrices defined in GenEO [33, 12] can be seen as a local SPSD splitting.

272 In [3], the authors highlight that the key idea to construct a coarse space relies  
 273 on the ability to identify the so-called local SPSD splitting matrices. They present  
 274 a class of algebraically constructed coarse spaces based on the local SPSD splitting  
 275 matrices. Moreover, this class can be extended to a larger variety of local SPSD  
 276 matrices. This extension has the advantage of allowing to construct efficient coarse  
 277 spaces for a multilevel structure in a practical way. This is discussed in the following  
 278 section.

279 **3. Extension of the class of coarse spaces.** In this section we extend the  
 280 class of coarse spaces presented in [3]. To do so, we present a class of matrices, that is  
 281 larger than the class of local SPSD splitting matrices. This will be our main building  
 282 block in the construction of efficient coarse spaces. Furthermore, this extension can  
 283 lead to a straightforward construction of hierarchical coarse spaces in a multilevel  
 284 Schwarz preconditioner setting.

285 **3.1. Extension of the class of local SPSD splitting matrices.** Regarding  
 286 the two-level additive Schwarz method, the authors of [3] introduced the local SPSD  
 287 splitting related to a subdomain as defined in (2.2). As it can be seen from the theory  
 288 presented in that paper, it is not necessary to have the exact matrices  $R_{j,I}AR_{j,I}^\top$ ,  
 289  $R_{j,I}AR_{j,\Gamma}^\top$ , and  $R_{j,\Gamma}AR_{j,I}^\top$  in the definition of the local SPSD splitting in order to  
 290 build an efficient coarse space. Indeed, the one and only necessary condition is to  
 291 define for each subdomain  $j$  an SPSD matrix  $\tilde{A}_j$  for  $j = 1, \dots, N$  such that:

$$292 \quad (3.1) \quad \begin{aligned} & R_{j,\Delta}\tilde{A}_j = 0, \\ & u^\top \sum_{j=1}^N \tilde{A}_j u \leq k u^\top A u, \forall u \in \mathbb{R}^n, \end{aligned}$$

294 where  $k$  is a number that depends on the local SPSD matrices  $\tilde{A}_j$  for  $j = 1, \dots, N$ .  
 295 The first condition means that  $\tilde{A}_j$  has the local SPSD structure associated with sub-  
 296 domain  $j$ , i.e., it has the following form:

$$297 \quad \mathcal{P}_j \tilde{A}_j \mathcal{P}_j^\top = \begin{pmatrix} \tilde{A}_{I,\Gamma}^j & 0 \\ 0 & 0 \end{pmatrix},$$

298 where  $\tilde{A}_{I,\Gamma}^j \in \mathbb{R}^{n_j \times n_j}$ . The second condition is associated with the stable decom-  
 299 position property [36, 12]. Note that with regard to the local SPSD matrices, the  
 300 authors in [33] only use these two conditions. That is to say, with matrices that verify  
 301 conditions (3.1) the construction of the coarse space is straightforward through the  
 302 theory presented in either [33] or [3]. To this end, we define in the following the local  
 303 SPSD (LSPSD) matrix associated with subdomain  $j$  as well as the associated local  
 304 filtering subspace that contributes to the coarse space.

305 **DEFINITION 3.1 (local SPSD matrices).** *An SPSD matrix  $\tilde{A}_{i,j} \in \mathbb{R}^{n_i \times n_i}$  is called*  
 306 *local SPSD (LSPSD) with respect to subdomain  $j$  if*

- 307 •  $R_{i,j,\Delta}\tilde{A}_{i,j} = 0$ ,
  - 308 •  $u^\top \sum_{j=1}^{N_i} \tilde{A}_{i,j} u \leq k_i u^\top A_i u$ ,
- 309 where  $k_i > 0$ .

310 We note that the local SPSD splitting matrices form a subset of the local SPSD  
 311 matrices.

312 **3.2. Multilevel coarse spaces.** This section summarizes the steps to be per-  
 313 formed in order to construct the coarse space at level  $i$  once we have the LSPSD  
 314 matrices associated with each subdomain at that level.

315 **DEFINITION 3.2** (coarse space based on LSPSD matrices). *Let  $\tilde{A}_{i,j} \in \mathbb{R}^{n_i \times n_i}$  for*  
 316  *$j = 1, \dots, N_i$  be LSPSD matrices. Let  $D_{i,j} \in \mathbb{R}^{n_{i,j}}$  for  $j = 1, \dots, N_i$  be the partition*  
 317 *of unity. Let  $\tau_i > 0$  be a given number. For a subdomain  $j \in \llbracket 1; N_i \rrbracket$ , let*

$$318 \quad G_{i,j} = D_{i,j} (R_{i,j} A_i R_{i,j}^\top) D_{i,j}.$$

319 *Let  $\tilde{P}_{i,j}$  be the projection on  $\text{range}(R_{i,j} \tilde{A}_j R_{i,j}^\top)$  parallel to  $\ker(R_{i,j} \tilde{A}_j R_{i,j}^\top)$ . Let  $K_{i,j} =$*   
 320  *$\ker(R_{i,j} \tilde{A}_{i,j} R_{i,j}^\top)$ . Consider the generalized eigenvalue problem:*

$$321 \quad (3.2) \quad \begin{aligned} \tilde{P}_{i,j} G_{i,j} \tilde{P}_{i,j} u_{i,j,k} &= \lambda_{i,j,k} R_{i,j} \tilde{A}_{i,j} R_{i,j}^\top u_{i,j,k}, \\ (u_{i,j,k}, \lambda_{i,j,k}) &\in \text{range}(R_{i,j} \tilde{A}_{i,j} R_{i,j}^\top) \times \mathbb{R}. \end{aligned}$$

323 *Set*

$$324 \quad (3.3) \quad Z_{i,j} = K_{i,j} \oplus \text{span}\{u_{i,j,k} \mid \lambda_{i,j,k} > \tau_i\}.$$

325 *Then, the coarse space associated with LSPSD matrices  $\tilde{A}_{i,j}$  for  $j = 1, \dots, N_i$  at level  $i$*   
 326 *is defined as:*

$$327 \quad (3.4) \quad \mathcal{S}_i = \bigoplus_{j=1}^{N_i} R_{i,j}^\top D_{i,j} Z_{i,j}.$$

328 *Following notations from [section 1](#), the columns of  $V_i$  span the coarse space  $\mathcal{S}_i$ . The*  
 329 *matrix  $A_{i+1}$  is defined as:*

$$330 \quad (3.5) \quad A_{i+1} = V_i^\top A_i V_i.$$

331 The local SPSD splitting matrices at level 1 will play an important role in the  
 332 construction of the LSPSD matrices at subsequent levels. In the following, we present  
 333 an efficient approach for computing LSPSD matrices for levels greater than 1.

334 **4. Partitioning for levels strictly greater than 1.** In this section, we ex-  
 335 plain how to obtain the partitioning sets  $\Omega_{i,j,I}$  for  $(i,j) \in \llbracket 2; L \rrbracket \times \llbracket 1; N_i \rrbracket$ . Once the  
 336 sets  $\Omega_{i,j,I}$  for  $j = 1, \dots, N_i$  are defined at level  $i$ , the following elements are readily  
 337 available: sets  $\Gamma_{i,j}$ ,  $\Delta_{i,j}$ , and  $\Omega_{i,j}$ ; restriction operators  $R_{i,j,I}$ ,  $R_{i,j,\Gamma}$ ,  $R_{i,j,\Delta}$ , and  $R_{i,j}$ ;  
 338 permutation matrices  $\mathcal{P}_{i,j}$  for  $j = 1, \dots, N_i$ . The partition of unity is constructed in  
 339 an algebraic way. The  $m$ th diagonal element of  $D_{i,j}$  is 1 if  $m \leq n_{i,j,I}$  and 0 otherwise.

340 **4.1. Superdomains as unions of several subdomains.** In this section, we  
 341 introduce the notion of a *superdomain*. It refers to the union of several neighboring  
 342 subdomains. Let  $\mathcal{G}_{i,1}, \dots, \mathcal{G}_{i,N_{i+1}}$  be disjoint subsets of  $\llbracket 1; N_i \rrbracket$ , where  $\bigcup_{j=1}^{N_{i+1}} \mathcal{G}_{i,j} =$   
 343  $\llbracket 1; N_i \rrbracket$ . We call the union of the subdomains  $\{k \in \llbracket 1; N_i \rrbracket : k \in \mathcal{G}_{i,j}\}$  superdomain  $j$ ,  
 344 for  $j = 1, \dots, N_{i+1}$ . [Figure 4.1](#) gives an example of how to set superdomains. Though  
 345 this definition of superdomains may look somehow related to the fine mesh, it is in  
 346 practice done at the algebraic level, as explained later on. Note that the indices of  
 347 columns and rows of  $A_{i+1}$  are associated with the vectors contributed by the subdo-  
 348 mains at level  $i$  in order to build the coarse space  $\mathcal{S}_i$ , see [Figure 4.2](#). Hence, defining  
 349 subdomains on the structure of  $A_{i+1}$  is natural once we have the subsets  $\mathcal{G}_{i,j}$ , for  
 350  $j = 1, \dots, N_{i+1}$ .

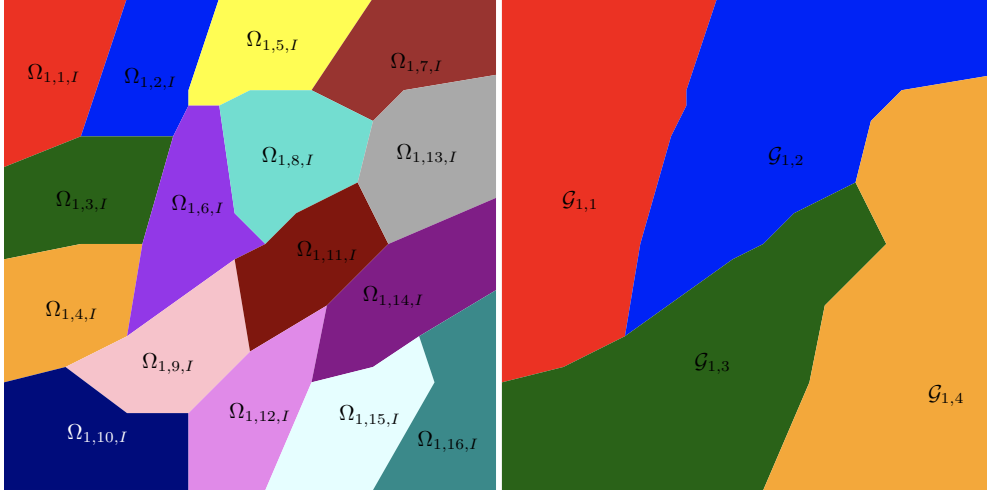


FIG. 4.1. Left: 16 subdomains at level 1. Right: 4 superdomains at level 1.  $\mathcal{G}_{1,j} = \llbracket 4(j-1) + 1; 4(j-1) + 4 \rrbracket$ .

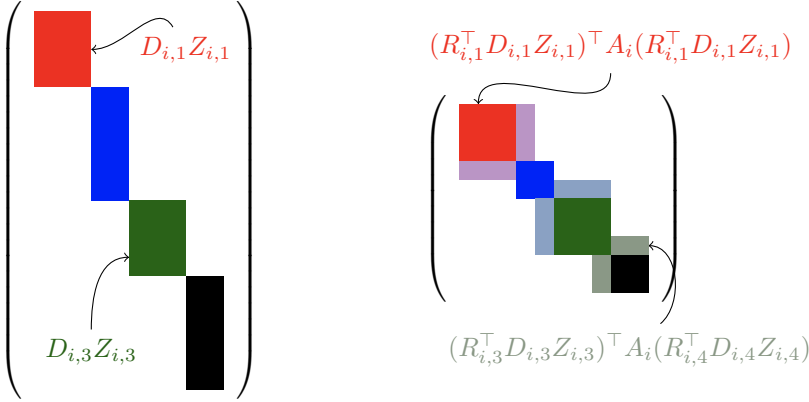


FIG. 4.2. Illustration of the correspondence of indices between the columns of  $V_i$  (left) and the rows and columns of  $A_{i+1}$  (right). Having no overlap in  $V_i$  is possible through a non-overlapping partition of unity.

351 **4.2. Heritage from superdomains.** Let  $e_{i,j}$  be the set of indices of the vectors  
 352 that span  $R_{i,j}^\top D_{i,j} Z_{i,j}$  in the matrix  $V_i$  for some  $(i, j) \in \llbracket 1; L-1 \rrbracket \times \llbracket 1; N_i \rrbracket$ , see  
 353 Figure 4.2. We define  $\Omega_{i+1,j,I} = \cup_{k \in \mathcal{G}_{i,j}} e_{i,k}$ , for  $j = 1, \dots, N_{i+1}$ . We denote  $\Omega_{i+1,j,\Gamma}$   
 354 the subset of  $\llbracket 1; n_{i+1} \rrbracket \setminus \Omega_{i+1,j,I}$  whose elements are at distance 1 from  $\Omega_{i+1,j,I}$  through  
 355 the graph of  $A_{i+1}$ . We note that

$$356 \quad \Omega_{i+1,j,\Gamma} \subset \bigcup_{p \in \mathcal{G}_{i,j}} \bigcup_{k \in \mathcal{V}_{i,p}} e_{i,k},$$

357 where  $\mathcal{V}_{i,j}$  represents the set of subdomains that are neighbors of subdomain  $j$  at  
 358 level  $i$  for  $j = 1, \dots, N_i$ . The overlapping subdomain  $j$  is defined by the set  $\Omega_{i+1,j} =$   
 359  $[\Omega_{i+1,j,I}, \Omega_{i+1,j,\Gamma}]$ . The rest of the sets, restriction, and prolongation operators can  
 360 be defined as given in section 1.

361 **5. LSPSD matrices for levels strictly greater than 1.** In [33, 12, 3], differ-  
 362 ent methods are suggested to obtain local SPSSD splitting matrices at level 1. These  
 363 matrices are used to construct efficient two-level additive Schwarz preconditioners.  
 364 Here in this section, we do not discuss the construction of these matrices at level 1. We  
 365 suppose that we have the local SPSSD matrices  $\tilde{A}_{1,j} \in \mathbb{R}^{n_1 \times n_1}$  for  $j = 1, \dots, N_1$ . We  
 366 focus on computing LSPSD matrices  $\tilde{A}_{i,j} \in \mathbb{R}^{n_i \times n_i}$  for  $(i, j) \in \llbracket 2; L \rrbracket \times \llbracket 1; N_i \rrbracket$ . We also  
 367 suppose that the coarse space  $\mathcal{S}_1$  is available, i.e., the matrices  $V_1$  and  $A_2 = V_1^\top A_1 V_1$   
 368 are known explicitly.

369 **PROPOSITION 5.1.** *Let  $i$  be a fixed level index, and let  $\tilde{A}_{i,j}$  be an LSPSSD of  $A_i$ ,*  
 370 *(see Definition 3.1), associated with subdomain  $j$ , for  $j = 1, \dots, N_i$ . Let  $\mathcal{G}_{i,1}, \dots, \mathcal{G}_{i,N_{i+1}}$*   
 371 *be a set of superdomains at level  $i$  associated with the partitioning at level  $i + 1$ , see*  
 372 *subsection 4.1. Let  $V_i^\top$  be the restriction matrix to the coarse space at level  $i$ . Then,*  
 373 *the matrix  $\tilde{A}_{i+1,j}$  which is defined as:*

$$374 \quad \tilde{A}_{i+1,j} = \sum_{k \in \mathcal{G}_{i,j}} V_i^\top \tilde{A}_{i,k} V_i,$$

375 *satisfies the conditions in Definition 3.1. That is,  $\tilde{A}_{i+1,j}$  is LSPSSD of  $A_{i+1}$  with*  
 376 *respect to subdomain  $j$  for  $j = 1, \dots, N_{i+1}$ .*

377 *Proof.* To prove that  $\tilde{A}_{i+1,j}$  is LSPSSD of  $A_{i+1}$  with respect to subdomain  $j$ , we  
 378 have to prove the following:

- 379 •  $R_{i+1,j,\Delta} \tilde{A}_{i+1,j} = 0$
- 380 •  $u^\top \sum_{j=1}^{N_{i+1}} \tilde{A}_{i+1,j} u \leq k_{i+1} u^\top A_{i+1} u$  for all  $u \in \mathbb{R}^{n_{i+1}}$ .

381 First, note that  $R_{i,k} \tilde{A}_{i,j} = 0$  for all non-neighboring subdomains  $k$  of subdomain  $j$ .  
 382 This yields  $Z_{i,k}^\top D_{i,k} R_{i,k} \tilde{A}_{i,j} = 0$  for these subdomains  $k$ .

383 Now, let  $m \in \llbracket 1; n_{i+1} \rrbracket \setminus \Omega_{i+1,j}$ . We will show that the  $m$ th row of  $\tilde{A}_{i+1,j}$  is zero.  
 384 Following the partitioning of subdomains at level  $i + 1$ , there exists a subdomain  $\Omega_{p_0}$   
 385 such that the  $m$ th column of  $V_i$  is part of  $R_{i,p_0}^\top D_{i,p_0} Z_{i,p_0}$ . We denote this column  
 386 vector by  $v_m$ . Furthermore, the subdomain  $p_0$  is not a neighbor of any subdomain  
 387 that is a part of the superdomain  $\mathcal{G}_{i,j}$ . Hence,  $v_m^\top \tilde{A}_{i,k} = 0$  for  $k \in \mathcal{G}_{i,j}$ . The  $m$ th row  
 388 of  $\tilde{A}_{i+1,j}$  is given as  $v_m^\top \sum_{k \in \mathcal{G}_{i,j}} \tilde{A}_{i,k} V_i$ . Then,  $v_m^\top \sum_{k \in \mathcal{G}_{i,j}} \tilde{A}_{i,k} = 0$ , and the  $m$ th row  
 389 of  $\tilde{A}_{i+1,j}$  is zero.

390 To prove the second condition, we have

$$391 \quad u^\top \sum_{j=1}^{N_{i+1}} \tilde{A}_{i+1,j} u = u^\top \sum_{j=1}^{N_{i+1}} \sum_{k \in \mathcal{G}_{i,j}} V_i^\top \tilde{A}_{i,k} V_i u.$$

393 Since  $\{\mathcal{G}_{i,j}\}_{1 \leq j \leq N_{i+1}}$  form a disjoint partitioning of  $\llbracket 1; N_i \rrbracket$ , we can write

$$394 \quad u^\top \sum_{j=1}^{N_{i+1}} \tilde{A}_{i+1,j} u = u^\top \sum_{k=1}^{N_i} V_i^\top \tilde{A}_{i,k} V_i u,$$

$$395 \quad = u^\top V_i^\top \sum_{k=1}^{N_i} \tilde{A}_{i,k} V_i u.$$

397  $\tilde{A}_{i,k}$  is an LSPSD matrix of  $A_i$  for  $k = 1, \dots, N_i$ . Hence, we have

$$398 \quad u^\top \sum_{j=1}^{N_{i+1}} \tilde{A}_{i+1,j} u \leq k_i u^\top V_i^\top A_i V_i u,$$

$$400 \quad \leq k_i u^\top A_{i+1} u.$$

401 We finish the proof by setting  $k_{i+1} = k_i$ .  $\square$

402 **Figure 5.1** gives an illustration of the LSPSD construction provided by **Proposition 5.1**. **Figure 5.1** (top left) represents the matrix  $A_1$ . The graph of  $A_1$  is partitioned into 16 subdomains. Each subdomain is represented by a different color. **Figure 5.1** (top right) represents the matrix  $V_1$  whose column vectors form a basis of the coarse space  $\mathcal{S}_1$ . Colors of columns of  $V_1$  correspond to those of subdomains in  $A_1$ . **Figure 5.1** (bottom left) represents the matrix  $A_2 = V_1^\top A_1 V_1$ . Note that column and row indices of  $A_2$  are associated with column indices of  $V_1$ . Four subdomains are used at level 2. The partitioning at level 2 is related to the superdomain  $\mathcal{G}_{1,j} = \llbracket 4(j-1)+1; 4(j-1)+4 \rrbracket$  for  $j = 1, \dots, 4$ . **Figure 5.1** (bottom right) represents an LSPSD matrix of  $A_2$  with respect to subdomain 1 at level 2.

412 **Theorem 5.2** shows that the third condition of the fictitious subspace lemma **Lemma 2.1** holds at level  $i$  for  $i = 1, \dots, L$ .

414 **THEOREM 5.2.** *Let  $\tilde{A}_{i,j}$  be an LSPSD of  $A_i$  associated with subdomain  $j$ , for*  
 415  *$(i, j) \in \llbracket 1; L \rrbracket \times \llbracket 1; N_i \rrbracket$ . Let  $\tau_i > 0$ ,  $Z_{i,j}$  be the subspace associated with  $\tilde{A}_{i,j}$ , and*  
 416  *$P_{i,j}$  be the projection on  $Z_{i,j}$  as defined in **Lemma 2.5**. Let  $u_i \in \mathbb{R}^{n_i}$  and let  $u_{i,j} =$*   
 417  *$(D_{i,j} (I_{n_{i,j}} - P_{i,j}) R_{i,j} u_i)$  for  $(i, j) \in \llbracket 1; L \rrbracket \times \llbracket 1; N_i \rrbracket$ . Let  $u_{i,0}$  be defined as,*

$$418 \quad u_{i,0} = (V_i^\top V_i)^{-1} V_i^\top \left( \sum_{j=1}^{N_i} R_{i,j}^\top D_{i,j} P_{i,j} R_{i,j} u_i \right).$$

419 Let  $m_i = (2 + (2k_{i,c} + 1)k_i \tau_i)^{-1}$ . Then,

$$420 \quad u_i = \sum_{j=0}^{N_i} R_{i,j}^\top u_{i,j},$$

421 and

$$422 \quad (5.1) \quad m_i \sum_{j=0}^{N_i} u_{i,j}^\top R_{i,j} A_i R_{i,j}^\top u_{i,j} \leq u_i^\top A_i u_i.$$

423 *Proof.* We have

$$424 \quad \sum_{j=0}^{N_i} R_{i,j}^\top u_{i,j} = V_i (V_i^\top V_i)^{-1} V_i^\top \left( \sum_{j=1}^{N_i} R_{i,j}^\top D_{i,j} P_{i,j} R_{i,j} u_i \right) + \sum_{j=1}^{N_i} R_{i,j}^\top u_{i,j}$$

425

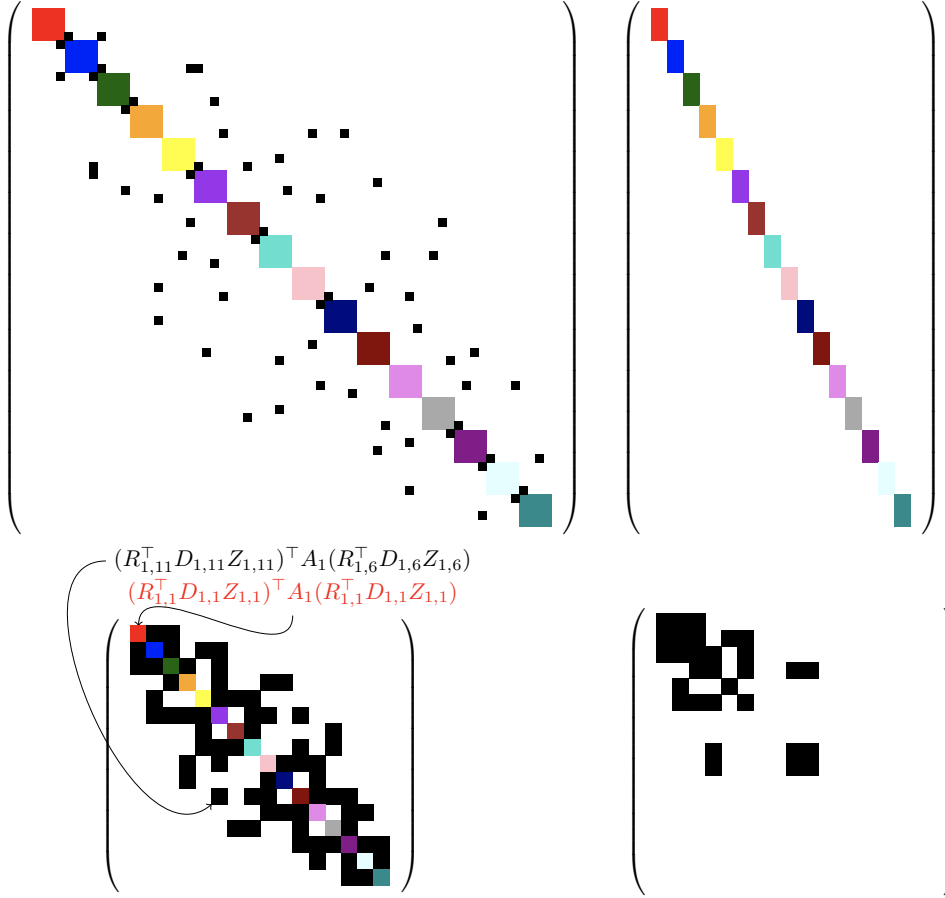


FIG. 5.1. Illustration of the LSPSD construction provided by [Proposition 5.1](#). Top left: the matrix  $A_1$ , top right:  $V_1$ , bottom left: the matrix  $A_2 = V_1^\top A_1 V_1$ , bottom right:  $\hat{A}_{2,1} = \sum_{j \in \mathcal{G}_{1,1}} V_1^\top \hat{A}_{1,j} V_1$ , where  $\mathcal{G}_{1,1} = 1, \dots, 4$

426 Since for all  $y \in \mathcal{S}_i$ ,  $V_i (V_i^\top V_i)^{-1} V_i^\top y = y$ , we have

$$\begin{aligned}
 427 \quad \sum_{j=0}^{N_i} R_{i,j}^\top u_{i,j} &= \sum_{j=1}^{N_i} R_{i,j}^\top D_{i,j} P_{i,j} R_{i,j} u_i + \sum_{j=1}^{N_i} R_{i,j}^\top (D_{i,j} (I_{n_{i,j}} - P_{i,j}) R_{i,j} u_i), \\
 428 \quad &= \sum_{j=1}^{N_i} R_{i,j}^\top D_{i,j} R_{i,j} u_i, \\
 430 \quad &= u_i.
 \end{aligned}$$

431 To prove the inequality [\(5.1\)](#), we start with the inequality from [Lemma 2.4](#). We  
 432 have

$$433 \quad (5.2) \quad \sum_{j=0}^{N_i} u_{i,j}^\top R_{i,j} A_i R_{i,j}^\top u_{i,j} \leq 2u_i^\top A_i u_i + (2k_{i,c} + 1) \sum_{j=1}^{N_i} u_{i,j}^\top R_{i,j} A_i R_{i,j}^\top u_{i,j},$$

435 where we chose  $u_{\mathcal{B}_i}$  in [Lemma 2.4](#) to be  $(u_{i,j})_{j=0, \dots, N_i}$  and  $u_{A_i} = u_i$ . In [Definition 3.2](#),

436 we defined  $Z_{i,j}$ , such that for all  $w \in \mathbb{R}^{n_{i,j}}$  we have

$$437 \quad ((I_{n_{i,j}} - P_{i,j})w)^\top (D_{i,j}R_{i,j}A_iR_{i,j}^\top D_{i,j}) ((I_{n_{i,j}} - P_{i,j})w) \leq \tau_i w^\top (R_{i,j}\tilde{A}_{i,j}R_{i,j}^\top) w. \\ 438$$

439 Hence, in the special case  $w = R_{i,j}u_i$ , we can write

$$440 \quad ((I_{n_{i,j}} - P_{i,j})R_{i,j}u_i)^\top (D_{i,j}R_{i,j}A_iR_{i,j}^\top D_{i,j}) ((I_{n_{i,j}} - P_{i,j})R_{i,j}u_i) \\ 441 \quad \leq \tau_i (R_{i,j}u_i)^\top (R_{i,j}\tilde{A}_{i,j}R_{i,j}^\top) (R_{i,j}u_i). \\ 442 \\ 443$$

444 Equivalently,

$$445 \quad u_{i,j}^\top R_{i,j}A_iR_{i,j}^\top u_{i,j} \leq \tau_i (R_{i,j}u_i)^\top R_{i,j}\tilde{A}_{i,j}R_{i,j}^\top (R_{i,j}u_i). \\ 446$$

447 Plugging this inequality in (5.2) gives

$$448 \quad \sum_{j=0}^{N_i} u_{i,j}^\top R_{i,j}A_iR_{i,j}^\top u_{i,j} \leq 2u_i^\top A_i u_i + (2k_{i,c} + 1) \tau_i \sum_{j=1}^{N_i} (R_{i,j}u_i)^\top R_{i,j}\tilde{A}_{i,j}R_{i,j}^\top (R_{i,j}u_i). \\ 449$$

450 Since  $\tilde{A}_{i,j}$  is local, we have

$$451 \quad (R_{i,j}u_i)^\top R_{i,j}\tilde{A}_{i,j}R_{i,j}^\top (R_{i,j}u_i) = u_i^\top \tilde{A}_{i,j}u_i, \text{ for } j = 1, \dots, N_i.$$

452 By using the fact that  $\tilde{A}_{i,j}$  is LSPSD of  $A_i$  for  $j = 1, \dots, N_i$ , we obtain the following:

$$453 \quad \sum_{j=0}^{N_i} u_{i,j}^\top R_{i,j}A_iR_{i,j}^\top u_{i,j} \leq 2u_i^\top A_i u_i + (2k_{i,c} + 1) k_i \tau_i u_i^\top A_i u_i. \\ 454$$

455 Multiplying both sides with  $m_i$  ends the proof, i.e.,

$$456 \quad m_i \sum_{j=0}^{N_i} u_{i,j}^\top R_{i,j}A_iR_{i,j}^\top u_{i,j} \leq u_i^\top A_i u_i. \quad \square \\ 457$$

458 In [3], the authors presented the minimal subspace that replaces  $Z_{i,j}$  (defined in (3.3)  
459 and used in Theorem 5.2) that is required to prove Theorem 5.2. The main difference  
460 with respect to the subspace that we define in (3.3) is that it is not necessary to include  
461 the entire kernel of the LSPSD matrix,  $K_{i,j}$ , in  $Z_{i,j}$ , see Definition 3.2. Nevertheless,  
462 in this work, we include the entire kernel of the LSPSD matrix in the definition of  
463  $Z_{i,j}$ . This allows us to ensure that the kernels of Neumann matrices are transferred  
464 across the levels, see Theorem 5.4. And in addition, this corresponds to the definition  
465 used in GenEO [12, Lemma 7.7] and to its implementation in the HPDDM library  
466 [19].

467 Theorem 5.3 provides an upper bound on the condition number of the preconditioned  
468 matrix  $M_i^{-1}A_i$  for  $i = 1, \dots, L$ .

469 THEOREM 5.3. *Let  $M_i$  be the additive Schwarz preconditioner at level  $i$  combined  
470 with the coarse space correction induced by  $\mathcal{S}_i$  defined in (3.4). The following inequality  
471 holds,*

$$472 \quad \kappa(M_i^{-1}A_i) \leq (k_{i,c} + 1) (2 + (2k_{i,c} + 1)k_i\tau_i).$$

473 *Proof.* Lemma 2.2, Lemma 2.3, and Theorem 5.2 prove that the multilevel preconditioner verifies the conditions in Lemma 2.1 at each level  $i$ . Hence, the spectrum of the preconditioned matrix  $M_i^{-1}A_i$  is contained in the interval  $[(2 + (2k_{i,c} + 1)k_i\tau_i)^{-1}, k_{i,c} + 1]$ . Equivalently, the condition number of the preconditioned matrix at level  $i$  verifies the following inequality

$$478 \quad \kappa(M_i^{-1}A_i) \leq (k_{i,c} + 1)(2 + (2k_{i,c} + 1)k_i\tau_i). \quad \square$$

479 Proposition 5.1 shows that the constant  $k_i$  associated with the LSPSD matrices at level  $i$  is independent of the number of levels and bounded by the number of subdomains at level 1. Indeed,

$$482 \quad k_1 \geq k_i \text{ for } i = 2, \dots, L.$$

483 Furthermore, in the case where the LSPSD matrices at the first level are the Neumann matrices,  $k_i$  is bounded by the maximum number of subdomains at level 1 that share an unknown.

484 The constant  $k_{i,c}$  for  $i = 1, \dots, L$  is the minimum number of distinct colors so that  $\{span\{R_{i,j}^\top\}\}_{1 \leq j \leq N_i}$  of the same color are mutually  $A_i$ -orthogonal. Both constants  $k_i$  and  $k_{i,c}$  are independent of the number of subdomains for each level  $i$ .

485 The constant  $\tau_i$  can be chosen such that the condition number of the preconditioned system at level  $i$  is upper bounded by a prescribed value. Hence, this allows to have a robust convergence of the preconditioned Krylov solver at each level.

486 Algorithm 5.1 presents the construction of the multilevel additive Schwarz method by using GenEO. The algorithm iterates over the levels. At each level, three main operations are performed. First, the construction of the LSPSD matrices. At level 1, the LSPSD matrices are the Neumann matrices, otherwise, Proposition 5.1 is used to compute them. Once the LSPSD matrix is available, the generalized eigenvalue problem in (3.2) has to be solved concurrently. Given the prescribed upper bound on the condition number,  $Z_{i,j}$  can be set. Finally, the coarse space is available and the coarse matrix is assembled.

487 The following Theorem 5.4, describes how the kernel of Neumann matrices are transferred across the levels.

488 THEOREM 5.4. *Suppose that  $\tilde{A}_{1,j}$  is the Neumann matrix associated with the subdomain  $\Omega_{1,j}$  for  $j \in \llbracket 1; N_1 \rrbracket$ . For  $(i, j) \in \llbracket 2; L \rrbracket \times \llbracket 1; N_i \rrbracket$ , let*

- 489 •  $\tilde{A}_{i,j}$  be the LSPSD matrices associated with  $A_{i,j}$  defined in Proposition 5.1,
- 490 •  $\mathcal{G}_{i-1,j}$  be the corresponding superdomains,
- 491 •  $\mathcal{G}_{i-1,j}^1$  be the union of subdomains at level 1 which contribute hierarchically to obtain  $\mathcal{G}_{i-1,j}$ ,
- 492 •  $\tilde{A}_{\mathcal{G}_{i-1,j}}$  be the Neumann matrix associated with  $\mathcal{G}_{i-1,j}^1$  (seeing  $\mathcal{G}_{i-1,j}^1$  as a subdomain),
- 493 •  $A_{\mathcal{G}_{i-1,j}}$  be the restriction of  $A$  to the subdomain  $\mathcal{G}_{i-1,j}^1$ .

494 Then, the kernel of  $\tilde{A}_{\mathcal{G}_{i-1,j}}$  is included in the kernel of  $\left(\prod_{l=1}^{i-1} V_l\right) \tilde{A}_{i,j} \left(\prod_{l=1}^{i-1} V_l\right)^\top$ .

495 *Proof.* First, note that for any LSPSD matrix computed as in Proposition 5.1, we have

$$\left(\prod_{l=1}^{i-1} V_l\right) \tilde{A}_{i,j} \left(\prod_{l=1}^{i-1} V_l\right)^\top = \left(\prod_{l=1}^{i-1} V_l\right) \left(\prod_{l=1}^{i-1} V_l\right)^\top \sum_{k \in \mathcal{G}_{i,j}^1} \tilde{A}_{1,k} \left(\prod_{l=1}^{i-1} V_l\right) \left(\prod_{l=1}^{i-1} V_l\right)^\top.$$



**Algorithm 5.1** Multilevel GenEO

**Require:**  $A_1 = A \in \mathbb{R}^{n \times n}$  SPD,  $L + 1$  number of levels,  $N_i$  number of subdomains at each level,  $\mathcal{G}_{i,j}$  sets of superdomains

**Ensure:** preconditioner at each level  $i$ ,  $M_i^{-1}$  with bounded condition number of  $M_i^{-1}A_i$

- 1: **for**  $i = 1, \dots, L$  **do**
- 2:   **for** each subdomain  $j = 1, \dots, N_i$  **do**
- 3:      $A_{i,j} = R_{i,j}A_iR_{i,j}^\top$  (local matrix associated with subdomain  $j$ )
- 4:     **if**  $i = 1$  **then**
- 5:       local SPSD  $\tilde{A}_{i,j}$  is Neumann matrix of subdomain  $j$
- 6:     **else**
- 7:       compute local SPSD matrix as

$$\tilde{A}_{i,j} = \sum_{k \in \mathcal{G}_{i,j}} V_{i-1}^\top \tilde{A}_{i-1,k} V_{i-1}$$

- 8:     **end if**
- 9:     solve the generalized eigenvalue problem (3.2), set  $Z_{i,j}$  as in (3.3)
- 10:    **end for**
- 11:     $S_i = \bigoplus_{j=1}^{N_i} D_{i,j}R_{i,j}^\top Z_{i,j}$ ,  $V_i$  basis of  $S_i$
- 12:    coarse matrix  $A_{i+1} = V_i^\top A_i V_i$ ,  $A_{i+1} \in \mathbb{R}^{n_{i+1} \times n_{i+1}}$
- 13: **end for**
- 14:  $M_i^{-1} = V_i A_{i+1}^{-1} V_i^\top + \sum_{j=1}^{N_i} R_{i,j}^\top A_{i,j}^{-1} R_{i,j}$

Moreover, due to the fact that  $\tilde{A}_{\mathcal{G}_{i-1,j}}$  and  $\tilde{A}_{1,k}$  are Neumann matrices, we have

$$u^\top \tilde{A}_{\mathcal{G}_{i-1,j}} u \leq u^\top \sum_{k \in \mathcal{G}_{i,j}^1} \tilde{A}_{1,k} u \leq k_1 u^\top \tilde{A}_{\mathcal{G}_{i-1,j}} u.$$

512 On one hand, the kernels of  $\tilde{A}_{1,k}$  for  $k \in \mathcal{G}_{i,j}^1$  are included, by construction, in the image  
 513 of  $V_1$ , see Definition 3.2. So is their intersection which is the kernel of  $\sum_{k \in \mathcal{G}_{i,j}^1} \tilde{A}_{1,k}$ .

514 On the other hand, the previous two-sided inequality implies that the kernels of  $\tilde{A}_{\mathcal{G}_{i-1,j}}$   
 515 and  $\sum_{k \in \mathcal{G}_{i,j}^1} \tilde{A}_{1,k}$  are identical. Hence, the kernel of  $\tilde{A}_{\mathcal{G}_{i-1,j}}$  is included in the image  
 516 of  $QQ^\top$ , where  $Q = \left(\prod_{l=1}^{i-1} V_l\right)$ .  $\square$

517 **Theorem 5.4** proves that the kernel of the Neumann matrix of a union of subdomains  
 518 at level 1 that hierarchically contribute to form a subdomain at level  $i$  is conserved by  
 519 the construction of the hierarchical coarse spaces. For example in the case of linear  
 520 elasticity, it is essential to include the rigid body motions in the coarse space in order  
 521 to have a fast convergence. As these are included in the kernel of the Neumann matrix  
 522 of the subdomain, the hierarchical coarse space includes them, consequently.

523 **6. Numerical experiments.** In this section, the developed theory is validated  
 524 numerically with FreeFEM [14] for finite element discretizations and HPDDM [19]  
 525 for domain decomposition methods. We present numerical experiments on two highly  
 526 challenging problems illustrating the efficiency and practical usage of the proposed  
 527 method. For both problems, we use  $N_1 = 2,048$  MPI processes (equal to the number  
 528 of subdomains at level 1), and the domain partitioning is performed using ParMETIS

529 [22], with no control on the alignments of subdomain interfaces. We compare the  
 530 two-level GenEO preconditioner and its multilevel extension by varying  $N_2$  between 4  
 531 and 256. For the two-level method,  $N_2$  corresponds to the number of MPI processes  
 532 that solve the coarse problem in a distributed fashion using MKL CPARDISO [17].  
 533 For the multilevel method,  $N_3$  is set to 1, i.e., a three-level method is used. The goal  
 534 of these numerical experiments is to show that when one switches from a two-level  
 535 method with an exact coarse solver, to our proposed multilevel method, the number  
 536 of outer iterations is not impacted. Thus, three levels are sufficient. As an outer  
 537 solver, since all levels but the coarsest are solved approximately, the flexible GMRES  
 538 [31] is used. It is stopped when relative unpreconditioned residuals are lower than  
 539  $10^{-6}$ . Subdomain matrices  $\{A_{i,j}\}_{1 \leq i \leq 2, 1 \leq j \leq N_i}$  are factorized concurrently using MKL  
 540 PARDISO, and eigenvalue problems are solved using ARPACK [24]. In both, two-  
 541 and three-level GenEO, we factorize the local matrices  $A_{1,j}$  for  $j \in \llbracket 1; N_1 \rrbracket$  and solve  
 542 the generalized eigenvalue problems concurrently at the first level. For this reason,  
 543 we do not take into account the time needed for these two steps which are performed  
 544 without any communication between MPI processes. We compare the time needed  
 545 to assemble and factorize  $A_2$  in the two-level approach against the time needed to  
 546 assemble  $A_2$  and local SPSD matrices  $\tilde{A}_{2,j}$  for  $j \in \llbracket 1; N_2 \rrbracket$ , solve the generalized  
 547 eigenvalue problems concurrently on the second level, assemble, and factorize the  
 548 matrix  $A_3$  in the three-level approach. We also compare the time spent in the outer  
 549 Krylov solver during the solution phase. Readers interested by a comparison of the  
 550 efficiency of GenEO and multigrid methods such as GAMG [1] are referred to [18].  
 551 FreeFEM scripts used to produce the following results are available at the following  
 552 URL: <https://github.com/prj-/aldaas2019multi><sup>1</sup>.

553 **6.1. Diffusion test cases.** The scalar diffusion equation with highly heteroge-  
 554 neous coefficient  $\kappa$  is solved in  $[0, 1]^d$  ( $d = 2$  or  $3$ ). The strong formulation of the  
 555 equation is:

$$\begin{aligned} -\nabla \cdot (\kappa \nabla u) &= 1 && \text{in } \Omega, \\ u &= 0 && \text{on } \Gamma_D, \\ \frac{\partial u}{\partial n} &= 0 && \text{on } \Gamma_N. \end{aligned}$$

558 The exterior normal vector to the boundary of  $\Omega$  is denoted  $n$ .  $\Gamma_D$  is the subset  
 559 of the boundary of  $\Omega$  corresponding to  $x = 0$  in 2D and 3D.  $\Gamma_N$  is defined as the  
 560 complementary of  $\Gamma_D$  with respect to the boundary of  $\Omega$ . We discretize the equation  
 561 using  $\mathbb{P}_2$  and  $\mathbb{P}_4$  finite elements in the 3D and 2D test cases, respectively. The number  
 562 of unknowns is  $441 \times 10^6$  and  $784 \times 10^6$ , with approximately 28 and 24 nonzero  
 563 elements per row in the 3D and 2D cases, respectively. The heterogeneity is due  
 564 to the jumps in the diffusion coefficient  $\kappa$ , see Figure 6.1, which is modeled using  
 565 a combination of jumps and channels, cf. the file `coefficients.idp` from <https://github.com/prj-/aldaas2019multi>.  
 566

567 The results in two dimensions are reported in Table 6.1. The number of outer  
 568 iterations for both two- and three-level GenEO is 32. The size of the level 2 operator  
 569 is  $n_2 = 25 \times 2,048 = 51,200$ . In all numerical results, the number of eigenvectors per  
 570 subdomain, here 25, is fixed. This is because ARPACK cannot a priori compute all  
 571 eigenpairs below a certain threshold, and an upper bound has to be provided instead.

---

<sup>1</sup>note to reviewers: the repository is now public

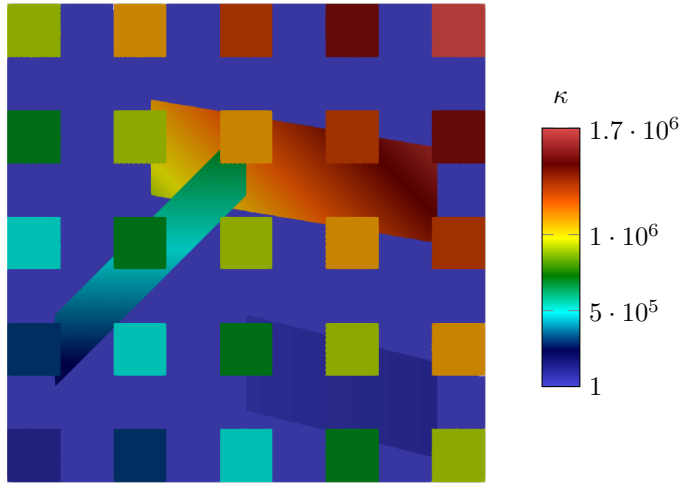


FIG. 6.1. Variation of the coefficient  $\kappa$  used for the diffusion test case

572 HPDDM is capable of filtering the eigenpairs for which eigenvalues are above the user-  
 573 specified GenEO threshold from [Lemma 2.5](#). However, this means that the coarse  
 574 operator may be unevenly distributed. With a fixed number of eigenvectors per sub-  
 575 domain, it is possible to use highly optimized uniform MPI routines and block matrix  
 576 formats. Hence, for performance reasons, all eigenvectors computed by ARPACK are  
 577 kept when building coarse operators. It is striking that the multilevel method does not  
 578 deteriorate the numerical performance of the outer solver. For the two-level method,  
 579 the first column corresponds to the time needed to assemble the Galerkin operator  $A_2$   
 580 from [\(3.5\)](#) (assuming  $V_1$  has already been computed by ARPACK), and to factorize it  
 581 using  $N_2$  MPI processes. For the three-level method, the first column corresponds to  
 582 the time needed to assemble level 2 local subdomain matrices  $\{A_{2,j}\}_{1 \leq j \leq N_2}$ , level 2  
 583 local SPSD matrices, solve the generalized eigenvalue problem [\(3.2\)](#) concurrently, as-  
 584 semble the Galerkin operator  $A_3$  and factorize it on a single process. The size of  
 585 the level 3 operator is  $n_3 = 20 \times N_2$ . For both two- and three-level methods, the  
 586 second column is the time spent in the outer Krylov solver once the preconditioner  
 587 has been set up. In the last column of the three-level method, the number of inner  
 588 iterations for solving systems involving  $A_2$ , which is not inverted exactly anymore,  
 589 is reported. For all tables, this column is an average over all successive outer iter-  
 590 ations. Another important numerical property of our method is that, thanks to fully  
 591 controlled bounds at each level, the number of inner iterations is low, independently  
 592 of the number of superdomains  $N_2$ . Because this problem is not large enough, it is  
 593 still tractable by a two-level method, for which HPDDM was highly optimized for.  
 594 Thus, there is no performance gain to be expected at this scale. However, one can  
 595 notice that the construction of the coarse operator(s) scales nicely with  $N_2$  for the  
 596 three-level method, whereas the performance of the direct solver MKL CPARDISO  
 597 quickly stagnates because of the finer and finer parallel workload granularity.

598 The results in three dimensions are reported in [Table 6.2](#). The number of outer  
 599 iterations for both the two- and three-level GenEO is 19. The observations made  
 600 in two dimensions still hold, and the dimensions of  $A_2$  and  $A_3$  are the same. Once  
 601 again, it is important to note that the number of outer iterations is the same for both  
 602 methods.

$N_2$	two-level GenEO			three-level GenEO			
	CS	solve	% of nnz $A_2$	CS	solve	inner it.	% of nnz $A_3$
4	2.4	11.9	0.19	6.5	27.4	14	56.0
16	1.8	11.3		3.6	15.4	15	19.0
64	1.9	12.1		3.0	16.7	14	5.5
256	2.4	18.4		2.8	13.9	13	1.4

TABLE 6.1  
Diffusion 2D test case, comparison between two- and three-level GenEO. The percentage of nonzero entries in  $A_1$  is 0.3%.

$N_2$	two-level GenEO			three-level GenEO			
	CS	solve	% of nnz $A_2$	CS	solve	inner it.	% of nnz $A_3$
4	7.0	20.9	0.36	16.9	43.6	17	62.0
16	5.0	19.8		7.7	26.7	17	28.0
64	5.1	20.1		5.8	32.7	15	8.9
256	5.2	24.1		5.3	22.6	14	2.6

TABLE 6.2  
Diffusion 3D test case, comparison between two- and three-level GenEO. The percentage of nonzero entries in  $A_1$  is 0.5%.

603 **6.2. Linear elasticity test cases.** The system of linear elasticity with highly  
 604 heterogeneous elastic moduli is solved in 2D and 3D. The strong formulation of the  
 605 equation is given as:

$$\begin{aligned}
 (6.1) \quad & \operatorname{div} \sigma(u) + f = 0 \quad \text{in } \Omega, \\
 & u = 0 \quad \text{on } \Gamma_D, \\
 & \sigma(u) \cdot n = 0 \quad \text{on } \Gamma_N.
 \end{aligned}$$

608 The physical domain  $\Omega$  is a beam of dimensions  $[0, 10] \times [0, 1]$ , extruded for  $z \in$   
 609  $[0, 1]$  in 3D. The Cauchy stress tensor  $\sigma(\cdot)$  is given by Hooke's law: it can be expressed  
 610 in terms of Young's modulus  $E$  and Poisson's ratio  $\nu$ .

$$\sigma_{ij}(u) = \begin{cases} 2\mu\varepsilon_{ij}(u) & i \neq j, \\ 2\mu\varepsilon_{ii}(u) + \lambda\operatorname{div}(u) & i = j, \end{cases}$$

612 where

$$\varepsilon_{ij}(u) = \frac{1}{2} \left( \frac{\partial u_i}{\partial x_j} + \frac{\partial u_j}{\partial x_i} \right), \mu = \frac{E}{2(1+\nu)}, \text{ and } \lambda = \frac{E\nu}{1-2\nu}.$$

614 The exterior normal vector to the boundary of  $\Omega$  is denoted  $n$ .  $\Gamma_D$  is the subset  
 615 of the boundary of  $\Omega$  corresponding to  $x = 0$  in 2D and 3D.  $\Gamma_N$  is defined as the  
 616 complementary of  $\Gamma_D$  with respect to the boundary of  $\Omega$ . We discretize (6.1) using  
 617 the following vectorial finite elements:  $(\mathbb{P}_2, \mathbb{P}_2, \mathbb{P}_2)$  in 3D and  $(\mathbb{P}_3, \mathbb{P}_3)$  in 2D. The  
 618 number of unknowns is  $146 \times 10^6$  and  $847 \times 10^6$ , with approximately 82 and 34  
 619 nonzero elements per row in the 3D and 2D cases, respectively. The heterogeneity is  
 620 due to the jumps in  $E$  and  $\nu$ . We consider discontinuous piecewise constant values  
 621 for  $E$  and  $\nu$ :  $(E_1, \nu_1) = (2 \times 10^{11}, 0.25)$ ,  $(E_2, \nu_2) = (10^7, 0.45)$ , see Figure 6.2.

622 Results in two (resp. three) dimensions are reported in Table 6.3 (resp. Table 6.4).  
 623 The number of outer iterations are 73 and 45 respectively. For these test cases, we

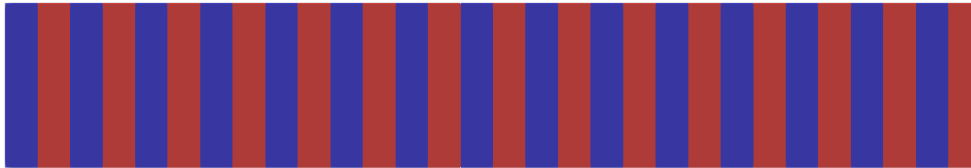


FIG. 6.2. Variation of the structure coefficients used for the elasticity test case

$N_2$	two-level GenEO			three-level GenEO			
	CS	solve	% of nnz $A_2$	CS	solve	inner it.	% of nnz $A_3$
4	4.8	52.7	0.18	22.5	179.3	31	43.0
16	3.9	50.3		9.3	124.9	57	17.0
64	4.0	53.1		7.2	71.5	34	4.9
256	4.8	63.2		6.8	71.2	44	1.4

TABLE 6.3  
Elasticity 2D test case, comparison between two- and three-level GenEO. The percentage of nonzero entries in  $A_1$  is 0.4%.

624 slightly relaxed the criterion for selecting eigenvectors in coarse spaces, which explains  
 625 why the iteration counts increase. However, the same observations as for the diffusion  
 626 test cases still hold. The dimension of the level 2 matrix is  $n_2 = 50 \times 2,048 = 1.02 \cdot 10^5$ ,  
 627 while for the level 3 matrix it is  $n_3 = 20 \times N_2$ . This means that 50 (resp. 20)  
 628 eigenvectors are kept per level 1 (resp. level 2) subdomains. We observe that the  
 629 number of iterations of the inner solver increases slowly when increasing the number  
 630 of subdomains from 4 to 256 in the 2D case and remains almost constant in the 3D  
 631 case. In terms of runtime, the two-level GenEO is faster than three-level GenEO for  
 632 these matrices of medium dimensions.

633 To show the potential of our method at larger scales, a three-dimensional linear  
 634 elasticity problem of size  $593 \times 10^6$  is now solved on  $N_1 = 16,384$  processes and  
 635  $N_2 = 256$  superdomains. With the two-level method,  $A_2$  is assembled and factorized  
 636 in 40.8 seconds. With the three-level method, this step now takes 35.1 seconds, see  
 637 Table 6.5. There is a two iterations difference in the iteration count. Not taking  
 638 into account the preconditioner setup, the problem is solved in 222.5 seconds in the  
 639 two-level case and 90.1 seconds in the multilevel case. In this test case the cost of  
 640 applying the two-level preconditioner on a given vector is approximately twice the cost  
 641 of applying the multilevel variant. At this regime, it is clear that there are important  
 642 gains for the solution phase. At even greater scales, gains for the setup phase are  
 643 also expected. Moreover, another interesting fact to note regarding computation time  
 644 is that the generalized eigenvalue problems solved concurrently at the first level to  
 645 obtain  $V_1$  actually represents a significant part of the total time of 377.6 seconds (resp.  
 646 244.8 seconds) with the two- (resp. three-)level method: 78.2 seconds. This cost can  
 647 be reduced by taking a larger number of (smaller) subdomains, with the drawback of  
 648 increasing the size of  $V_1$  and thus  $A_2$ . This drawback represents a clear bottleneck  
 649 for the two-level method but is alleviated by using the three-level method, making it  
 650 a good candidate for problems at greater scales.

651 **7. Conclusion.** In this paper, we reviewed general properties of overlapping  
 652 Schwarz preconditioners and presented a framework for its multilevel extension. We

$N_2$	two-level GenEO			three-level GenEO			
	CS	solve	% of nnz $A_2$	CS	solve	inner it.	% of nnz $A_3$
4	28.5	46.9	0.38	78.9	296.7	23	43.0
16	17.3	35.4		24.5	124.5	23	19.0
64	15.0	33.2		15.4	62.2	21	7.9
256	13.6	40.7		10.6	50.7	23	2.5

TABLE 6.4

Elasticity 3D test case, comparison between two- and three-level GenEO. The percentage of nonzero entries in  $A_1$  is 3.3%.

$N_2$	two-level GenEO		three-level GenEO		
	CS	solve	CS	solve	inner it.
256	40.8	222.5	35.1	90.1	11

TABLE 6.5

Elasticity 3D test case, comparison between two- and three-level GenEO

653 generalized the local SPSD splitting presented in [3] to cover a larger set of matrices  
654 leading to more flexibility for building robust coarse spaces. Based on local SPSD  
655 matrices on the first level, we presented how to compute local SPSD matrices for  
656 coarser levels. The multilevel solver based on hierarchical local SPSD matrices is  
657 robust and guarantees a bound on the condition number of the preconditioned matrix  
658 at each level depending on predefined values. Numerical experiments illustrate the  
659 theory and prove the efficiency of the method on challenging problems of large size  
660 arising from heterogeneous linear elasticity and diffusion problems with jumps in the  
661 coefficients of multiple orders of magnitude.

662 **8. Acknowledgments.** We would like to thank the anonymous referees for their  
663 comments and remarks that helped us improve the clarity of this manuscript. This  
664 work was granted access to the HPC resources of TGCC@CEA under the allocation  
665 A0050607519 made by GENCI. The work of the second author was supported by the  
666 NLAFFET project as part of European Union’s Horizon 2020 research and innovation  
667 program under grant 671633.

668

## REFERENCES

- 669 [1] M. F. ADAMS, H. H. BAYRAKTAR, T. M. KEAVENY, AND P. PAPADOPOULOS, *Ultrascaleable*  
670 *Implicit Finite Element Analyses in Solid Mechanics with over a Half a Billion Degrees of*  
671 *Freedom*, in Proceedings of the 2004 ACM/IEEE Conference on Supercomputing, SC ’04,  
672 IEEE Computer Society, 2004.
- 673 [2] M. F. ADAMS AND J. W. DEMMEL, *Parallel Multigrid Solver for 3D Unstructured Finite El-*  
674 *ement Problems*, in Proceedings of the 1999 ACM/IEEE Conference on Supercomputing,  
675 SC ’99, ACM, 1999.
- 676 [3] H. AL DAAS AND L. GRIGORI, *A class of efficient locally constructed preconditioners based on*  
677 *coarse spaces*, SIAM Journal on Matrix Analysis and Applications, 40 (2019), pp. 66–91.
- 678 [4] S. BADIA, A. MARTÍN, AND J. PRINCIPE, *Multilevel balancing domain decomposition at extreme*  
679 *scales*, SIAM Journal on Scientific Computing, 38 (2016), pp. C22–C52.
- 680 [5] P. E. BJØRSTAD, M. J. GANDER, A. LONELAND, AND T. RAHMAN, *Does SHERM for Additive*  
681 *Schwarz Work Better than Predicted by Its Condition Number Estimate?*, in International  
682 Conference on Domain Decomposition Methods, Springer, 2017, pp. 129–137.
- 683 [6] A. BORZI, V. DE SIMONE, AND D. DI SERAFINO, *Parallel algebraic multilevel Schwarz pre-*  
684 *conditioners for a class of elliptic PDE systems*, Computing and Visualization in Science, 16  
685 (2013), pp. 1–14.

- 686 [7] M. BREZINA, A. CLEARY, R. FALGOUT, V. HENSON, J. JONES, T. MANTEUFFEL, S. MCCORMICK,  
687 AND J. RUGE, *Algebraic Multigrid Based on Element Interpolation (AMGe)*, SIAM Journal  
688 on Scientific Computing, 22 (2001), pp. 1570–1592.
- 689 [8] X.-C. CAI AND M. SARKIS, *A restricted additive Schwarz preconditioner for general sparse*  
690 *linear systems*, SIAM Journal on Scientific Computing, 21 (1999), pp. 792–797.
- 691 [9] T. F. CHAN AND T. P. MATHEW, *Domain decomposition algorithms*, Acta Numerica, 3 (1994),  
692 pp. 61–143.
- 693 [10] T. CHARTIER, R. D. FALGOUT, V. E. HENSON, J. JONES, T. MANTEUFFEL, S. MCCORMICK,  
694 J. RUGE, AND P. S. VASSILEVSKI, *Spectral AMGe ( $\rho$ AMGe)*, SIAM Journal on Scientific  
695 Computing, 25 (2003), pp. 1–26.
- 696 [11] C. CHEVALIER AND F. PELLEGRINI, *PT-SCOTCH: A tool for efficient parallel graph ordering*,  
697 Parallel Computing, 34 (2008), pp. 318–331. Parallel Matrix Algorithms and Applications.
- 698 [12] V. DOLEAN, P. JOLIVET, AND F. NATAF, *An introduction to domain decomposition methods*,  
699 Society for Industrial and Applied Mathematics, 2015. Algorithms, theory, and parallel  
700 implementation.
- 701 [13] M. GRIEBEL AND P. OSWALD, *On the abstract theory of additive and multiplicative Schwarz*  
702 *algorithms*, Numerische Mathematik, 70 (1995), pp. 163–180.
- 703 [14] F. HECHT, *New development in FreeFem++*, Journal of Numerical Mathematics, 20 (2012),  
704 pp. 251–266.
- 705 [15] A. HEINLEIN, A. KLAWONN, O. RHEINBACH, AND F. RÖVER, *A Three-Level Extension of the*  
706 *GDSW Overlapping Schwarz Preconditioner in Three Dimensions*, technical report, Uni-  
707 versität zu Köln, November 2018.
- 708 [16] V. E. HENSON AND U. M. YANG, *BoomerAMG: A parallel algebraic multigrid solver and pre-*  
709 *conditioner*, Applied Numerical Mathematics, 41 (2002), pp. 155–177. Developments and  
710 Trends in Iterative Methods for Large Systems of Equations.
- 711 [17] INTEL, *MKL web page*. <https://software.intel.com/en-us/intel-mkl>, 2019.
- 712 [18] P. JOLIVET, *Domain decomposition methods. Application to high-performance computing*, the-  
713 ses, Université de Grenoble, Oct. 2014.
- 714 [19] P. JOLIVET, F. HECHT, F. NATAF, AND C. PRUD’HOMME, *Scalable domain decomposition pre-*  
715 *conditioners for heterogeneous elliptic problems*, in Proceedings of the International Con-  
716 ference on High Performance Computing, Networking, Storage and Analysis, SC13, ACM,  
717 2013.
- 718 [20] J. JONES AND P. VASSILEVSKI, *AMGe Based on Element Agglomeration*, SIAM Journal on  
719 Scientific Computing, 23 (2001), pp. 109–133.
- 720 [21] D. KALCHEV, C. LEE, U. VILLA, Y. EFENDIEV, AND P. VASSILEVSKI, *Upscaling of mixed finite*  
721 *element discretization problems by the spectral AMGe method*, SIAM Journal on Scientific  
722 Computing, 38 (2016), pp. A2912–A2933.
- 723 [22] G. KARYPIS AND V. KUMAR, *Multilevel k-way partitioning scheme for irregular graphs*, Journal  
724 of Parallel and Distributed Computing, 48 (1998), pp. 96–129.
- 725 [23] F. KONG AND X.-C. CAI, *A highly scalable multilevel Schwarz method with boundary geometry*  
726 *preserving coarse spaces for 3D elasticity problems on domains with complex geometry*,  
727 SIAM Journal on Scientific Computing, 38 (2016), pp. C73–C95.
- 728 [24] R. LEHOUCQ, D. SORENSEN, AND C. YANG, *ARPACK users’ guide: solution of large-scale*  
729 *eigenvalue problems with implicitly restarted Arnoldi methods*, vol. 6, Society for Industrial  
730 and Applied Mathematics, 1998.
- 731 [25] J. MANDEL, B. SOUSEDÍK, AND C. R. DOHRMANN, *Multispace and multilevel BDDC*, Comput-  
732 ing, 83 (2008), pp. 55–85.
- 733 [26] O. MARQUES, A. DRUINSKY, X. S. LI, A. T. BARKER, P. VASSILEVSKI, AND D. KALCHEV, *Tuning*  
734 *the coarse space construction in a spectral AMG solver*, Procedia Computer Science, 80  
735 (2016), pp. 212–221. International Conference on Computational Science 2016, ICCS 2016,  
736 6-8 June 2016, San Diego, California, USA.
- 737 [27] S. V. NEPOMNYASCHIKH, *Mesh theorems of traces, normalizations of function traces and their*  
738 *inversions*, Russian Journal of Numerical Analysis and Mathematical Modelling, 6 (1991),  
739 pp. 1–25.
- 740 [28] ———, *Decomposition and fictitious domains methods for elliptic boundary value problems*,  
741 1992.
- 742 [29] Y. NOTAY, *An aggregation-based algebraic multigrid method*, Electronic Transactions on Nu-  
743 merical Analysis, 37 (2010), pp. 123–146.
- 744 [30] C. PECHSTEIN, *Finite and boundary element tearing and interconnecting solvers for multiscale*  
745 *problems*, vol. 90, Springer Science & Business Media, 2012.
- 746 [31] Y. SAAD., *A Flexible Inner–Outer Preconditioned GMRES Algorithm*, SIAM Journal on Sci-  
747 entific Computing, 14 (1993), pp. 461–469.

- 748 [32] Y. SAAD, *Iterative Methods for Sparse Linear Systems*, Society for Industrial and Applied  
749 Mathematics, 2nd ed., 2003.
- 750 [33] N. SPILLANE, V. DOLEAN, P. HAURET, F. NATAF, C. PECHSTEIN, AND R. SCHEICHL, *Abstract*  
751 *robust coarse spaces for systems of PDEs via generalized eigenproblems in the overlaps*,  
752 *Numerische Mathematik*, 126 (2014), pp. 741–770.
- 753 [34] J. TOIVANEN, P. AVERY, AND C. FARHAT, *A multilevel feti-dp method and its performance for*  
754 *problems with billions of degrees of freedom*, *International Journal for Numerical Methods*  
755 *in Engineering*, 116 (2018), pp. 661–682.
- 756 [35] A. TOSELLI AND O. WIDLUND, *Domain Decomposition Methods - Algorithms and Theory*,  
757 *Springer Series in Computational Mathematics*, Springer Berlin Heidelberg, 2005.
- 758 [36] J. XU, *Theory of Multilevel Methods*, PhD thesis, Cornell University, 1989.
- 759 [37] S. ZAMPINI, *PCBDDC: A class of robust dual-primal methods in PETSc*, *SIAM Journal on*  
760 *Scientific Computing*, 38 (2016), pp. S282–S306.